

98-8



ОБЪЕДИНЕННЫЙ
ИНСТИТУТ
ЯДЕРНЫХ
ИССЛЕДОВАНИЙ

Дубна

98-8

E7-98-8

V.A.Karnaukhov, S.P.Avdeyev, W.D.Kuznetsov,
L.A.Petrov, V.K.Rodionov, A.S.Zubkevich, H.Oeschler¹,
O.V.Bochkarev², L.V.Chulkov², E.A.Kuzmin²,
A.Budzanowski³, W.Karcz³, M.Janicki³, E.Norbeck⁴,
A.S.Botvina⁵

MULTIFRAGMENTATION INDUCED
BY LIGHT RELATIVISTIC PROJECTILES
AND HEAVY IONS:
SIMILARITIES AND DIFFERENCES

Submitted to «Ядерная физика»

¹Institut für Kernphysik, TU Darmstadt, 64289, Germany

²Kurchatov Institute, 123182, Moscow, Russia

³H.Niewodniczanski Institute of Nuclear Physics, 31-342, Cracow, Poland

⁴University of Iowa, Iowa City, IA 52242 USA

⁵Institute for Nuclear Research, 117312, Moscow, Russia

1998

I. Thermal and dynamic multifragmentation

Nuclear fragmentation was discovered 60 years ago [1,2] in the cosmic rays studies as a puzzling phenomenon, when in the collisions of relativistic protons with a target nuclear fragments are emitted, whose masses are heavier than those of alpha particles, but lighter than those of fission fragments. Now they are called intermediate mass fragments (IMF, $2 \leq Z \leq 20$). Later on, in the 1950s, this phenomenon was observed in the experiments at the accelerators [3] and after that it was studied leisurely for three decades. The situation changed dramatically after 1982, when B. Jacobsson et al. discovered multiple emission of IMF in emulsion irradiated by ^{12}C (1030 MeV) at the CERN synchrocyclotron [4]. The experimental data stimulated appearance of a number of theoretical models, which related the copious production of IMF to the liquid-gas phase transition in nuclear matter. In a nucleus, as in usual liquid, peculiar conditions can be created (high temperature and reduced density), when system enters the region of phase instability (spinodal region). This state may disintegrate into an ensemble of small drops (IMF), surrounded by a nuclear gas (nucleons and helium nuclei).

The idea of getting a new insight into the problem of the nuclear equation of state stimulated great interest in the multifragmentation phenomenon in the middle of the 1980s. Around a dozen very complicated experimental devices were created to investigate this process by using heavy ion beams, which are well suited for producing extremely hot nuclei. But in this case heating of nuclei is accompanied by compression, strong rotation and shape distortion, which cause the so-called dynamic effects in the nuclear decay. It is difficult to disentangle all these effects to get information on the thermodynamic properties of a hot nuclear system. The picture becomes much clearer when light relativistic projectiles (protons, helium) are used. One should expect that dynamic effects are negligible in that case. An-

other advantage is that all the fragments are emitted by the only source — the target spectator. Its excitation energy is almost entirely thermal. So, the use of light relativistic projectiles is the way to observe and study thermal multifragmentation. The latest review of the problem is given in [5].

The interplay of thermal and "mechanical" excitations in the process of copious IMF emission was treated in a number of papers [e.g. 6,7]. Figure 1 shows a diagram calculated (except the dashed line) in [6] with the hydrodynamical approach and the percolation model. The IMF emission was considered for heated and compressed ^{208}Pb . The left lower corner of diagram is a domain of normal fragment evaporation, true multifragmentation (many-body decay) takes place above the line. Compression is as effective for multifragmentation as thermal excitation. Even the cold nucleus can disintegrate when the compressional energy is larger than 3.5 MeV/nucleon. The influence of rotation and shape distortion on the multifragmentation probability was analyzed in several papers (e.g. [7]). But compression is expected to be a more important dynamic property of the heavy ion collisions in that aspect. So, the reactions induced by relativistic light projectiles occupy only abscissae, as $E^*/A \simeq \varepsilon_T$, the domain of heavy ion collisions is all area of the diagram, as the excitation energy in that case is composed by the thermal and compressional energies: $E^*/A = \varepsilon_T + \varepsilon_C$. In fact, the threshold for thermal multifragmentation is lower than predicted in [6] (solid point in Fig. 1), so the actual border between the evaporation and multifragmentation regions is presented by the dashed line.

Up to now a great body of data has been accumulated, which gives a chance to analyze the similarities and differences of thermal and "dynamic" (with heavy ions) multifragmentation. This will be done considering the data on the mean IMF multiplicities, the fragment charge distributions, kinetic energy spectra and the time scale of IMF emission. In both cases it is proved that multifragmentation is the main decay mode for nuclei with excitation energy above the threshold of this decay channel.

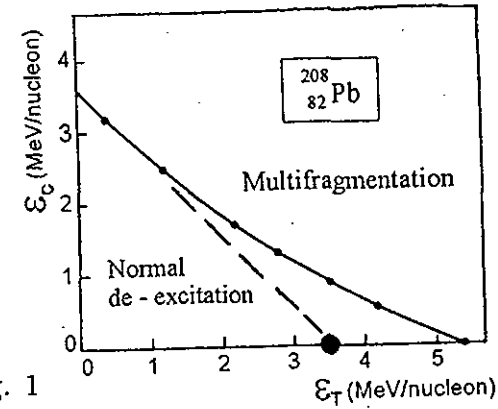


Fig. 1

Multifragmentation and normal de-excitation regions calculated for ^{208}Pb [6] as a function of the thermal and compressional energies per nucleon. The dot shows the experimentally estimated threshold for thermal multifragmentation of the target spectator for $p + \text{Au}$ collisions [8]

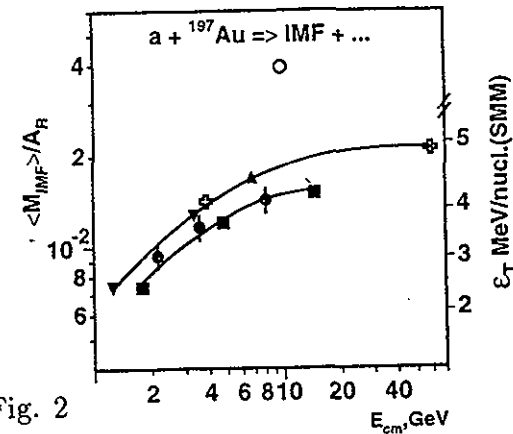


Fig. 2

Specific IMF multiplicity (for events with at least one IMF), for $a + \text{Au}$ collisions as a function of the c.m. energy of the system. Lower line: dots — proton beam, squares — ^3He and ^4He beams. Upper line is for heavy ion beams: ^{40}Ar , ^{36}Ar , ^{129}Xe , ^{12}C (inverse kinematics) and ^{197}Au . Open circle is for the central $\text{Au} + \text{Au}$ collisions, others points are inclusive data. The right scale gives the excitation energy according to SMM

II. IMF multiplicity

In this paper we define $\langle M \rangle$ as a mean IMF multiplicity for the events with emission of at least one IMF. The mean fragment multiplicity averaged over all inelastic collisions $\langle M^* \rangle$ is connected with $\langle M \rangle$ via the relation $\langle M^* \rangle = \langle M \rangle (1 - P(0))$, where $P(0)$ is the probability of the events without IMF emission. Thus $\langle M \rangle$ is never smaller than one.

Figure 2 presents a collection of some data on specific IMF mean multiplicities $\langle M \rangle / A_R$ (A_R is the mass number of the fragmenting nucleus) for collisions $a + Au$, where a ranges from relativistic protons [8] and He [8,9] to such a heavy projectile as ^{197}Au [10,11]. The data are shown as a function of the incident energy in the centre-of-mass system. There are no definite experimental data on the mass numbers of fragmenting nuclei except for peripheral $Au + Au$ collisions at 600 MeV/nucleon (the last point in Fig. 2) [12]. For the proton-induced fragmentation at beam energies of 2.16, 3.6 and 8.1 GeV, A_R values were found from the fit of data to the calculations in which the fast stage of the collisions was described by the intranuclear cascade model [13] with additional mass and energy loss during the thermal expansion phase (INC + Exp.) [8]. The disintegration of residuals was described in the framework of the Copenhagen statistical multifragmentation model (SMM) considering the decay of a diluted system at the freeze-out density $\rho_f \simeq \frac{1}{3}\rho_0$ [14]. For ^{40}Ar [15], ^{36}Ar [16], ^{129}Xe [17] beams, the mass numbers A_R were estimated on the assumption of the same mass loss in respect to the initial system as in the case of the proton-induced fragmentation (at the closest energy). For $Au + C$ collisions A_R was found by the same procedure as for $Au + Au$ peripheral collisions with regard for universality of spectator fragmentation at relativistic bombarding energies [10]. The solid points in Fig. 2 present the inclusive data (averaged over the entire range of the impact parameters). The open point is for the central $Au + Au$ collisions at 100 MeV/nucleon [11] with A_R estimated in that paper.

The inclusive data for specific IMF multiplicity for heavy ion collisions are only slightly larger than those for the fragmentation induced by relativistic light projectiles. The process is almost insensitive to reaction dynamics. This observation suggests that the energy transfer to the residual nucleus is the primary quantity controlling its decay. On the right scale of Fig. 2 the excitation energy per nucleon is plotted which, according to SMM, corresponds to the left scale of specific IMF multiplicity. This is the thermal excitation energy ε_T .

The relation between $\langle M \rangle / A_R$ and ε_T in the framework of SMM is shown in Fig. 3. As the input in calculating the curve, we used A_R , Z_R values and the excitation energies for residual nuclei produced by the INC code for $^4He + Au$ collisions at 14.6 GeV. The mean specific IMF multiplicity grows with the excitation energy up to the maximum value at ≈ 9 MeV/nucleon and after that it falls down because of switching on the vaporization regime. The right scale of Fig. 2 corresponds to the growing part of this dependence. The first three points (for peripheral $Au + C$ and $Au + Au$ collisions) are obtained from the data [10] for both multiplicity and excitation energy. They are located in accordance with the SMM prediction if we assume some reasonable contribution of collective energy (shown by arrows) to the excitation energy of the projectile spectator. Evidence for that will be demonstrated later when the fragment kinetic energies are considered.

The statistical multifragmentation model fails to describe the data for the most violent collisions of heavy ions. The open points in Fig. 3 are for central $Au + Au$ collisions at 100 MeV/nucleon [11] and at 250 MeV/nucleon [18] (mass number of source was taken to be equal 320). The radial flow energies, mainly caused by compression, are around 10 MeV/nucleon and 21.5 MeV/nucleon respectively, but they are subtracted from the total excitation energy to get the thermal one. The multiplicities are definitely larger than predicted by SMM. One should look for another mechanism of fragment formation in the overheated system than the one suggested by the statistical multifragmentation model.

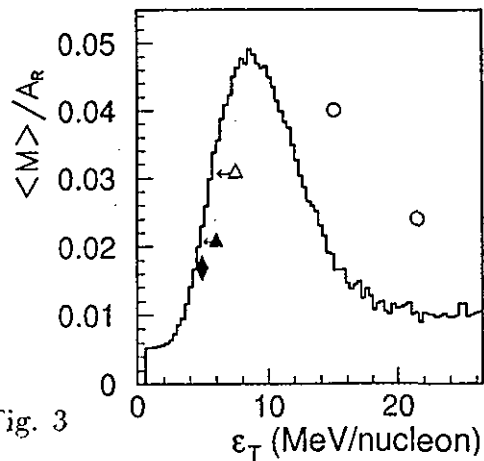


Fig. 3

Specific IMF multiplicity as a function of the thermal excitation energy. The curve is calculated by SMM. Experimental points: solid diamond and triangle are inclusive data for peripheral $^{12}C + Au$ and $Au + Au$ collisions at 600 MeV/nucleon, the open triangle — for $Au + Au$ (600 MeV/nucleon) collisions at $b/b_{max} = 0.6 - 0.75$, open circles are for central $Au + Au$ interactions at 100 and 250 MeV/nucleon

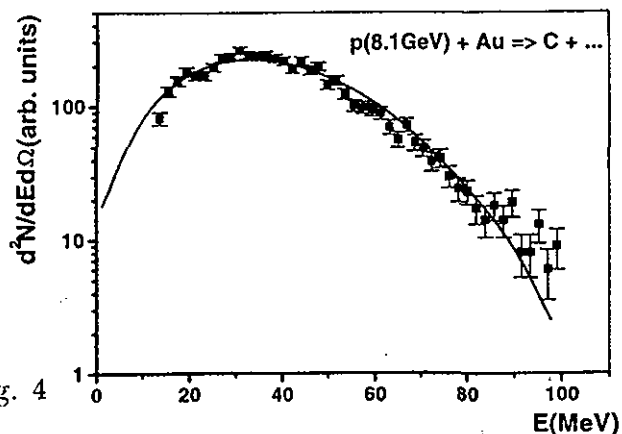


Fig. 4

Energy spectrum of carbon from the $p + Au$ collisions at 8.1 GeV compared with the SMM-calculation

III. Fragment kinetic energy spectra

As an example of a fragment energy spectrum for pure thermal multifragmentation, Fig. 4 presents the spectrum of carbon for $p + Au$ collisions at 8.1 GeV [8]. The line gives the result of calculations using the combined (INC + Expansion + SMM)-model. In our paper [19] it is shown that around 75% of the mean energy of carbon fragments are gained from the Coulomb acceleration and only a quarter is pure thermal. So, the mean fragment energy is sensitive to the size of the source (Z , A and R). The Z and A values are defined by the first two stages of the interaction (INC + Exp.). The parameters of the (INC + Exp.) calculations are not adjusted specially to fit energy spectra. Only one additional parameter was used in calculating the excitation energy and mass loss during the expansion stage to reach agreement between the calculated and measured IMF multiplicities [8]. The model considers the break-up of the hot expanded system assuming that the expansion velocity equals zero. If the expansion velocity is actually significant, it should manifest itself in the fragment energy spectra. It is invisible for the case presented in Fig. 4. Agreement between the data and the calculated curve is rather good and the upper limit of the expansion velocity at the break-up moment is less than $0.02 c$.

Figure 5 presents some collection of the data for the mean IMF energies per nucleon for collisions of different projectiles with the Au target: our data for protons (8.1 GeV) and 4He (3.65 GeV/nucleon) [8], ^{36}Ar (110 MeV/nucleon) [20], Au (600 MeV/nucleon), peripheral collisions [10], Au (100 MeV/nucleon and 150 MeV/nucleon), central collisions [11, 21]. For the proton and 4He beams the direct measurements are used at $\theta = 87^\circ$ in respect to the beam direction. For ^{36}Ar the data are obtained from the measurements of the fragment transverse energy. For the projectile spectator fragmentation in peripheral $Au + Au$ collisions energies are estimated from the transverse and longitudinal momentum width of IMF. For the central $Au + Au$ collisions the direct measurements of fragment energies and time of flight are used.

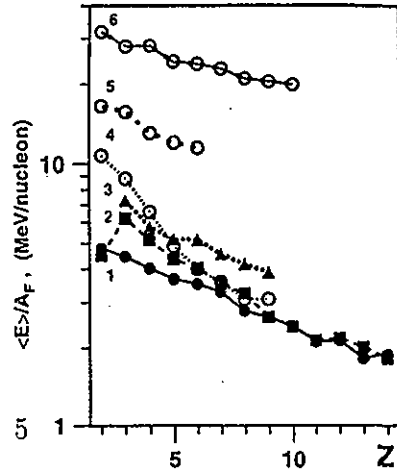


Fig. 5

IMF mean energies per nucleon (in center-of-mass system) for collisions of different projectiles with gold: 1 — p (8.1 GeV), 2 — ${}^4\text{He}$ (3.65 GeV/nucleon), 3 — ${}^{36}\text{Ar}$ (110 MeV/nucleon), 4 — Au (600 MeV/nucleon, peripheral coll.), 5 — Au (100 MeV/nucleon, central coll.), 6 — Au (150 MeV/nucleon, central coll.)

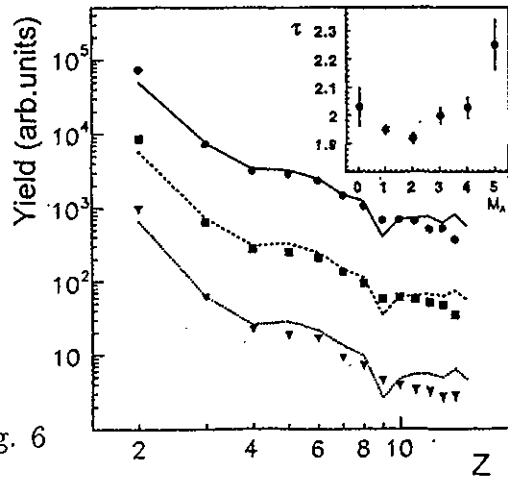


Fig. 6

Fragment charge distributions for the $p+\text{Au}$ collisions at 8.1 GeV (top), 3.6 GeV and 2.16 GeV (bottom). The lines are calculated by INC + Exp. + SMM (normalized at $Z = 3$). The insert gives τ -parameters deduced from the IMF charge spectra for a beam energy of 8.1 GeV as a function of the measured (associated) IMF multiplicity

For heavier projectiles the mean IMF energies are higher (even for ${}^4\text{He}$ beam) than those for the proton-induced collisions. They are dramatically higher for the central $\text{Au} + \text{Au}$ collisions and that cannot be caused by the larger source charge Z_s . It is estimated to be around 120 for an incident energy of 100 MeV/nucleon [11] and that can explain only a quarter of the enhancement in the IMF energies. In the main, this is explained by the effect of the radial flow initiated by significant compression of nuclear matter in the collision. For an incident energy of 150 MeV/nucleon of the Au beam the flow energy is found to be equal to 19.9 ± 2.3 MeV/nucleon from the analysis with the blast model, which gives good fit of the IMF energy spectra in the central collisions at 150-400 MeV/nucleon [18]. According to this analysis, around 60% of the available energy are stored in the radial flow.

The minor enhancement of the IMF mean energies in respect to those for $p + \text{Au}$ interaction, observed for ${}^4\text{He}$ - and ${}^{36}\text{Ar}$ - induced fragmentation, can also be attributed to the effect of collective flow which just comes to the game.

Dealing with peripheral $\text{Au} + \text{Au}$ collisions (curve 4), one should ask oneself how significant the contribution of the Coulomb field of the target spectator to the kinetic energy of the fragment originating from the projectile spectator is. The typical time for thermally driven expansion of the system before the break-up is around 50-70 fm/c. The separation of the target and the projectile spectators after that time (for an energy of 600 MeV/nucleon) is around 50 fm. At that distance the Coulomb field of the target is greatly reduced and it can hardly explain the enhancement of the fragment kinetic energies in respect to that for the proton-induced emission. Thus, this enhancement is most probably caused again by the effect of collective flow, which is rather modest compared to the central collisions.

IV. Fragment charge distributions

Figure 6 gives an example of charge distributions for the thermal multifragmentation induced in gold by relativistic protons. The data are well described by the calculations in the (INC + Expansion + SMM)-model. The general trend of the distributions follows the power law $Y(Z) \sim Z^{-\tau}$, yielding $\tau = 2.17 \pm 0.08$; 1.90 ± 0.06 and 1.93 ± 0.06 for beam energies of 2.16, 3.6 and 8.1 GeV respectively. The charge distributions are further studied by selecting different IMF multiplicities. The insert in Fig. 6 shows the dependence of the τ -parameter on the detected IMF multiplicity M_A for an incident energy of 8.1 GeV. With increasing multiplicity, the τ -parameter first decreases and then rises. In earlier papers on the multifragmentation [22] the power-law behaviour of the fragment charge yield and the observed minimum of the τ -parameter was interpreted as an indication of the proximity to the critical point for the liquid-gas phase transition in nuclear matter¹. But in fact, the fragmenting system is not so close to the critical point [23] and one should look for a less exotic explanation of the minimum of the τ -parameter also found here as a function of M_A . It is given by SMM with allowance for the secondary decay of excited fragments. As shown above, the IMF multiplicity is correlated with the excitation energy of the system. For low multiplicities the system is close to the evaporation regime. In this case increasing excitation energy results in enhancement of the yield of heavier fragments (τ decreases). As the excitation continues increasing, the secondary decay of the fragments becomes more significant, enhancing the yield of light fragments (τ rises). Quantitatively this is shown in Fig. 8.

A set of data on the charge distributions for fragments produced in the collisions of different projectiles with the gold target is given in Fig. 7. Distributions 1–4 are inclusive, obtained with the beams of protons (8.1 GeV) [8], ^{40}Ar (30 and 220 MeV/nucleon) [25] and ^{84}Kr (35 MeV/nucleon) [26]. Distribution 5 is measured for the peripheral $\text{Au} + \text{Au}$ collisions at 1000 MeV/nucleon [11]. All these distributions can be rendered by the power law. The similarity is remarkable. To

discuss the ability of the statistical multifragmentation model to fit the data, let us consider Fig. 8, which presents the comparison of the measured values for the exponent τ with the ones calculated by SMM as a function of the excitation (thermal) energy per nucleon. In these calculations Z , A and E^*/A of the system were generated by the INC code for the $^4\text{He} + \text{Au}$ collisions at 3.65 GeV/nucleon. The model-predicted charge distributions are well fitted by the power law for the excitation energies below 10 MeV/nucleon. For higher energies they become more like exponential ones. The calculated τ -value has a minimum at $E^*/A \simeq 4$ MeV/nucleon. First, consider the solid symbols. The circles are the data for $p + \text{Au}$ collisions for 2.16, 3.6 and 8.1 GeV (inclusive data). Here the mean excitation energies are obtained from the fit of the experimental mean IMF multiplicity and the SMM calculations. The diamonds are for $\text{Au} + \text{Au}$ peripheral collisions at 600 MeV/nucleon, excitation energies are estimated experimentally [10]. There is good agreement of the experimental points and calculations for excitation energies of up to 7 MeV/nucleon. The deviation for higher energies can be caused by the contribution of the collective flow to the estimated total excitation energy.

The open points in Fig. 8 are for ^{40}Ar (30 MeV/nucleon) and ^{84}Kr (35 MeV/nucleon) collisions with gold (inclusive data). The mean excitation energies are estimated on the basis of the systematics for the specific multiplicities (Fig. 2). The measured τ -values are lower than the minimal one calculated by SMM. But, as noted in [25], this can be explained by the enhancement of the yield of heavier IMF caused by another reaction mechanism — dissipative collisions (or multinucleon transfer).

Now, turn to Fig. 7. For the central $\text{Au} + \text{Au}$ collisions the charge distributions (6 and 7) are completely different from those just discussed. They are fitted by the exponential function $Y(Z) \sim \exp(-\alpha Z)$ with the parameter α increasing with incident energy. As was already mentioned, the statistical multifragmentation model predicts the exponential shape of the charge distribution of fragments if the thermal excitation energy exceeds 10 MeV/nucleon, but underestimates the IMF multiplicity. In the exhaustive paper [18] the

¹This prediction is corrected in the recent paper [24].

IMF charge distributions for $a + Au$ collisions. Projectiles:
 1 - p (8.1 GeV), 2 - Ar (30 MeV/nucleon), 3 - Kr (35 MeV/nucleon), 4 - Ar (220 MeV/nucleon), 5 - Au (1000 MeV/nucleon), peripheral, 6 - Au (100 MeV/nucleon) and 7 - Au (400 MeV/nucleon), central collisions

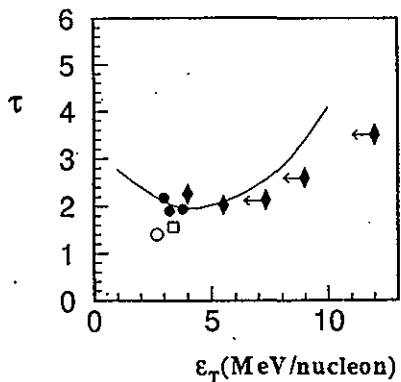
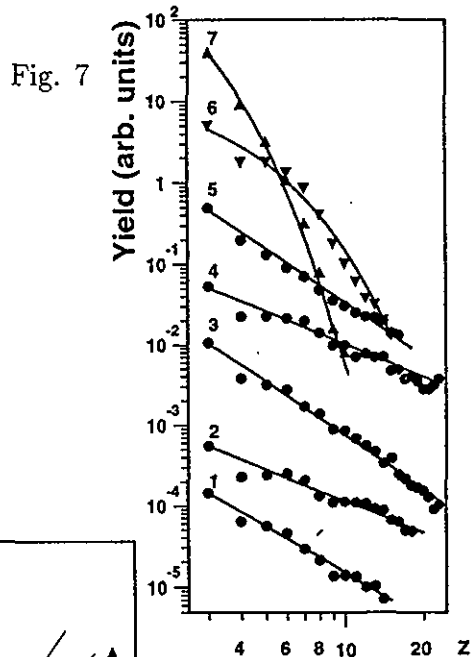


Fig. 8

Power parameter τ as a function of the excitation energy per nucleon. The line is calculated with SMM. Experimental data: solid circles are for $p + Au$ collisions at 2.16, 3.6 and 8.1 GeV; diamonds are for peripheral $Au + Au$ collisions at 600 MeV/nucleon (selected for different Z_{bound}); open symbols are for ^{40}Ar (30 MeV/nucleon) and ^{84}Kr (35 MeV/nucleon)

charge distributions for the central $Au + Au$ collisions at 150-400 MeV/nucleon are compared with the ones calculated by SMM, Quantum Statistical Model [27], statistical Model WIX [28]. None can render the experimental data significantly underestimating the yield of heavier IMF. The implementation of the microscopic Quantum Molecular Dynamic Model gives similar results. It is suggested that the higher cluster yield could be explained in the quasistatistical approach if the freeze-out density is around $0.8 \rho_0$ (the system is well outside the spinoidal region). This is a very bold idea, when it is remembered that the thermal excitation energy of the system exceeds the binding energy by several times (it is estimated in [18] to be 33 MeV/nucleon for $Au + Au$ collisions at 400 MeV/nucleon). As an alternative, this overheated system can be thought of as completely vaporized at the freeze-out moment. In that case coalescence (appropriately modified by collective flow) seems to be the proper mechanism of fragment formation from the gaseous phase. In [29] it was successfully applied to describe the data for the central $^{20}Ne + ^{238}U$ collisions at 0.25-2.1 GeV/nucleon.

V. On the time scale of IMF emission

The time scale of IMF emission is a crucial characteristic for understanding this decay mode: is it a "slow" sequential process of independent emission of IMF or is it a new (multibody) decay mode with "simultaneous" ejection of fragments governed by the total accessible phase space? Only the latter process is usually called "multifragmentation". "Simultaneous" means that all fragments are liberated during the time smaller than the characteristic one $\tau_c \approx 10^{-21}$ s, which is the mean time of the Coulomb acceleration [30]. For that case emission of IMF is not independent, they interact via Coulomb forces during the acceleration in the common electric field after freeze-out. To measure the emission time τ_{em} of IMF (i.e. the mean time between two successive fragment emissions) is a direct way to answer the question as to the nature of the multifragmentation phenomenon.

There are two procedures to measure the emission time: analysis of the IMF-IMF correlation function in respect to the relative velocity and in respect to the relative angle. An example of implementation of the second method is given in Fig. 9. It shows the IMF-IMF relative angle correlation for the fragmentation of the target spectator in ${}^4\text{He}$ (14.6 GeV) + Au collisions [19]. The correlation function exhibits a minimum at $\theta_{rel} = 0$ arising from the Coulomb repulsion between the coincident fragments. The magnitude of this effect drastically depends on the time scale of emission, since the longer the time distance between the fragments, the larger their space separation and the weaker the Coulomb repulsion. The multibody Coulomb trajectory calculations fit the data on the assumption that the mean emission time τ_{em} is less than 75 fm/c ($2.3 \cdot 10^{-22}\text{s}$). This value is considerably smaller than the characteristic Coulomb time τ_c . The trivial mechanism of multiple IMF emission (independent evaporation) is excluded.

Figure 10 gives some collection of the experimental data for the mean time of IMF emission for the collisions of different projectiles with the gold target [19, 31-37]. For the incident energies lower than 1.5 GeV the measured values of τ_{em} are larger than the Coulomb correlation time and fragment emission should be classified as an evaporation process. For higher beam energies all the data are in favour of a true multifragmentation mechanism. It should be remembered that for thermal multifragmentation (or quasithermal one, with moderate collective energy) the IMF emission takes place after expansion bringing the system into the spinoidal region. According to different model calculations it takes 50–70 fm/c. So the full time scale of the process also includes that expansion time. For the central Au + Au collisions the disintegration time is determined dynamically by the radial flow velocity [37] which reaches 0.33 c for the 400 MeV/nucleon incident energy [18].

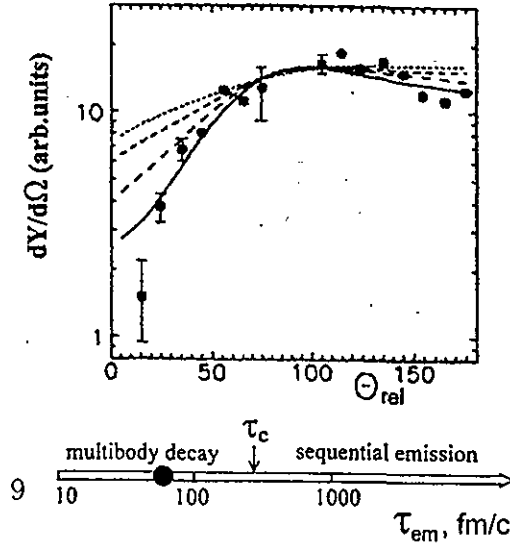


Fig. 9

Distribution of relative angles between coincident IMF for the ${}^4\text{He}$ (14.6 GeV) + Au collisions. The lines are calculated for the mean emission times (from bottom) 0, 100, 400 and 800 fm/c

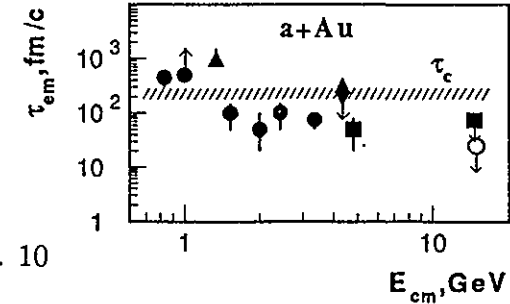


Fig. 10

IMF emission times for $a + \text{Au}$ collisions as a function of the center-of-mass energy of the system. The dashed line corresponds to the Coulomb correlation time. Solid dots — Ar beam, triangle — ${}^{18}\text{O}$, diamond — ${}^{56}\text{Fe}$, squares — ${}^3\text{He}$ and ${}^4\text{He}$ beams, open point — central Au + Au collisions

VI. Conclusion

The relativistic light projectiles are a more adequate tool for investigating thermal multifragmentation as the excitation energy of the target spectator is almost entirely thermal one. In that case all the observables (IMF multiplicities, fragment kinetic energy spectra, charge yields and some correlation data) are well described by the Statistical Multifragmentation Model, which considers the fast multibody decay of the expanded (and thermally equilibrated) hot nucleus. For heavy ion collisions, heating of a nucleus is accompanied by compression and rotation. When the thermal excitation energy is less than 10 MeV/nucleon and compression is modest, the statistical interpretation seems to be applicable. The mean fragment multiplicities and charge distributions are in agreement with the statistical model calculations (even for peripheral $Au + Au$ collisions). But the fragment kinetic energies are enhanced by the collective flow.

The situation is completely different for central $Au + Au$ collisions, when an overheated ($\epsilon_T > 10$ MeV/nucleon) and well-compressed system is created. The statistical models fail to render the basic observable of the process — the fragment yields, giving considerably lower values. The fragment kinetic energies are dynamic in origin. They are mostly determined by the collective flow caused by the initial compression. The huge collective flow makes questionable the implementation of global thermodynamical concepts in describing such violent collisions.

The authors are thankful to Profs A. Hryniewicz, A.M. Baldin, S.T. Belyaev, N.A. Russakovich for their support and to W. Trautmann for fruitful discussions. The research was supported in part by Grant No. 96-02-18952 from the Russian Foundation for Basic Research, by Grant No. 94-2249 from INTAS, by Grant No. P30B 09509 from the Polish State Committee for Scientific Research, by Contract No. 06DA453 with Bundesministerium für Forschung und Technologie and by the US National Science Foundation.

References

1. Gurevich, I.I. et al., Dokl. Akad. Nauk SSSR, 1938, vol. 18, p. 169.
2. Schopper, E., Naturwissenschaften, 1937, vol. 25, p. 557.
3. Lozhkin, O.V., Perfilov N.A., Zh. Eksp. Teor. Fiz., 1956, vol. 31, p. 913.
4. Jacobsson, B. et al., Z. Phys. A, 1982, vol. 307, p. 293.
5. Moretto, L.G., Wozniak, G.J., Ann. Rev. Nucl. Part. Sci., 1993, vol. 43, p. 379.
6. Desbois, J. et al., Z. Phys. A, 1987, vol. 328, p. 101.
7. De Paula, L. et al., Phys. Lett. B, 1991, vol. 258, p. 251.
8. Avdeyev, S.P. et al., JINR Rapid Comm., 1997, vol. 82, p. 71; Avdeyev, S.P., et al., submitted to European Physics Review.
9. Foxford, E.R. et al., Phys. Rev. C, 1996, vol. 54, p. 749; Moreley, K.B. et al., ibid. p. 737.
10. Schüttauf, A. et al., Nucl. Phys. A, 1996, vol. 607, p. 457.
11. Kunde, G.J. et al., Phys. Rev. Lett., 1995, vol. 74, p. 38; Hsi, W.C., Phys. Rev. Lett., 1994, vol. 73, p. 3367.
12. Pochodzalla, J. et al., Phys. Rev. Lett., 1995, vol. 75, p. 1040.
13. Toneev, V.D., Gudima, K.K., Nucl. Phys. A, 1983, vol. 400, p. 173c.
14. Bondorf, J.P., et al., Phys. Rep., 1995, vol. 257, No 3, p. 134.
15. Trockel, R. et al., Phys. Rev. C, 1989, vol. 39, p. 729.
16. de Souza, R.T. et al., Phys. Lett. B, 1991, vol. 268, p. 6.
17. Bownann, D.R. et al., Phys. Rev. C, 1992, vol. 46, p. 1834.
18. Reisdorf, W. et al., Nucl. Phys. A, 1997, vol. 612, p. 493.
19. Schmakov, S.Yu. et al., Phys. At. Nucl., 1995, vol. 58, p. 1635; Lips, V. et al., Phys. Lett. B, 1994, vol. 338, p. 141.
20. de Souza, R.T. et al., Phys. Lett. B, 1993, vol. 300, p. 29.
21. Jeong, S.C. et al., Phys. Rev. Lett., 1994, vol. 72, p. 3468.
22. Siemens, P.J., Nature, 1983, vol. 305, p. 410; Panagiotou, A.D. et al., Phys. Rev. Lett., 1984, vol. 52, p. 496.
23. Karnaukhov, V.A., Phys. At. Nucl., 1997, vol. 60, No 10, p. 1625.
24. Schmelzer, J. et al., Phys. Rev. C, 1997, vol. 55, p. 1917.
25. Milkau, U. et al., Phys. Rev. C, 1991, vol. 44, p. R1242.
26. Milkau, U. et al., Z. Phys. A, 1993, vol. 346, p. 227.
27. Konopka, J. et al., Phys. Rev. C, 1994, vol. 50, p. 2085.
28. Randrup, J., Comput. Phys. Commun., 1993, vol. 77, p. 77.

29. Gosset, J. et al., Phys. Rev. C, 1977, vol. 16, p. 629.
30. Shapiro, O., Gross, D.H.E., Nucl. Phys. A. 1994, vol. 573, p. 143.
31. Zhi Yong He et al., Nucl. Phys. A, 1997, vol. 620, p. 214.
32. Louvel, M. et al., Phys. Lett. B, 1994, vol. 320, p. 221.
33. Pochodzalla, J., GSI Report 91-11, Darmstadt, 1991.
34. Fox, D. et al., Phys. Rev. C, 1993, vol. 47, p. R421.
35. Sangster, T.C. et al., Phys. Rev. C, 1993, vol. 47, p. R2457.
36. Wang, G. et al., INC-40007-119, Indiana University, Bloomington, 1997.
37. Kämpfer, B. et al., Phys. Rev. C, 1993, vol. 48, p. R955.

Received by Publishing Department
on January 26, 1998.